

LASER INTERFEROMETER GRAVITATIONAL WAVE  
OBSERVATORY

**-LIGO-**

CALIFORNIA INSTITUTE OF TECHNOLOGY  
MASSACHUSETTS INSTITUTE OF TECHNOLOGY

Document Type	DCC Number 050251	August 19, 2005
<b>Measuring the Long-Term Drift of the Mode Cleaner Length</b>		
Ian Duke, Valera Frolov		

Distribution of this draft: LIGO scientists  
This is an internal working note of the LIGO Laboratory

**California Institute of Technology**  
**LIGO Project – MS 18-33**  
**Pasadena, CA 91125**  
Phone (626) 395-2129  
Fax (626) 304-9834  
E-mail: [info@ligo.caltech.edu](mailto:info@ligo.caltech.edu)

**Massachusetts Institute of Technology**  
**LIGO Project – MS 20B-145**  
**Cambridge, MA 01239**  
Phone (617) 253-4824  
Fax (617) 253-7014  
E-mail: [info@ligo.mit.edu](mailto:info@ligo.mit.edu)

www: <http://www.ligo.caltech.edu/>

## ABSTRACT

**Variation in the length of the mode cleaner cavity causes the RF sidebands to shift away from resonance. This results in oscillator phase noise appearing as amplitude modulation in the transmitted light. We measure drift in the length of the mode cleaner on the scale of several weeks and determine if it is necessary to correct the sideband modulation frequency or the cavity length to minimize this amplitude noise. The measurement is performed by imposing an additional audio frequency modulation of the carrier beam before it enters the RF electro-optic modulator. The magnitude and phase of the beat signal in the mode cleaner transmitted beam give the length and direction of the offset. We also investigate the effect of mode cleaner cavity length variation on oscillator phase noise contributing to RF amplitude modulation in the light coming out of the mode cleaner.**

## METHOD

The measurement involves taking the transfer function from an excitation of the VCO input to the REFL-Q channel with a single bounce off the recycling mirror (no IFO). We connected the PSL AWG channel 3 to the excitation B channel of the mode cleaner board, which then passes to the VCO input of the FSS. Using the DTT from the control room, we inject a 633 Hz signal that modulates the carrier frequency before it enters the EOM. This produces audio sidebands around both the carrier and the 25 MHz resonant sidebands.

If the mode cleaner length differs from the RF sideband resonant length, the excitation will produce a beat signal in the MC transmitted beam (see Appendix). The light is picked up at the LSC REFL photo detector and the signal in the REFL-Q channel is demodulated at the RF oscillator frequency. A sine-sweep is used to measure the transfer function in the 630-635 Hz range. After correcting for the DC intensity of the light on the photodiode, the magnitude of the transfer function gives the length of the offset and the phase gives the direction. The measurement is done with 1W of power into the MC.

For length changes on the scale with which this project is concerned (hundreds of microns), the magnitude of the transfer function varies linearly with the change in length of the MC cavity. We calibrate the measurement using HEPI to actively change the cavity length. The HEPI offset is stepped in increments of 100  $\mu\text{m}$  and the transfer function is measured at each point. We apply a linear fit to the data and use the parameters of the fit as a calibration for subsequent daily measurements.

The results of the calibration were confirmed by replacing the crystal oscillator with a signal generator and modulating the RF sidebands only. We sweep the RF sideband frequency about the nominal value and measure the transfer function to the REFL-AC channel. A sign change in the phase of the transfer function designates the cavity resonant frequency, which is easily related to the length of the cavity.

## RESULTS

In performing the first calibration on June 16, we found that the mode cleaner was about 300  $\mu\text{m}$  longer than the 25 MHz sideband resonance length. This was verified with a frequency sweep using a signal generator to drive the EOM. The sweep indicated a 750 Hz shift from resonance.

The calibration was repeated on June 29<sup>th</sup> and again on July 11<sup>th</sup>. The June 29<sup>th</sup> calibration confirmed a drift of approximately 90 $\mu\text{m}$  drift during the first two weeks of measurement. The frequency sweep performed on the same day showed an offset of  $\sim$ 450 Hz from sideband resonance. The parameters of each fit are shown in Table 1.

Calibration Date	Slope	Zero Crossing
June 16	$1.9 \pm 0.05 \times 10^{-3} \mu\text{m}^{-1}$	$-290 \pm 8 \mu\text{m}$
June 29	$2.1 \pm 0.05 \times 10^{-3} \mu\text{m}^{-1}$	$-200 \pm 5 \mu\text{m}$
July 11	$2.6 \pm 0.03 \times 10^{-3} \mu\text{m}^{-1}$	$-193 \pm 2 \mu\text{m}$

**Table 1 - Parameters of the Linear Fit to Calibration Data. The loop gain was changed between the June 29 and July 11 measurements.**

Measurements were taken twice daily (morning and afternoon) through mid-August except during power outages or when the interferometer was in use. The results of these daily measurements are shown in Figure 1. The largest drift occurred between June 17<sup>th</sup> and July 5<sup>th</sup>, during which the MC cavity became shorter by about 150  $\mu\text{m}$ . Since July 11<sup>th</sup>, the cavity length has remained the same to within about 20  $\mu\text{m}$ .

## POSSIBLE SOURCES OF DRIFT

We investigated two possible sources of drift in the mode cleaner length, thermal expansion and motion of the optics relative to the frame.

Change in the LVEA temperature is likely to explain the 100-150  $\mu\text{m}$  drift that took place over the first three weeks of measurement. During the last week of May, an error in the calibration of thermometers in the LVEA caused the temperature to rise to 70-72°F [1]. Beginning June 16th the sensors were recalibrated and the LVEA temperature was reduced by 0.5-1°F per day until it reached 68°F, consistent with the conditions of the S4 run.

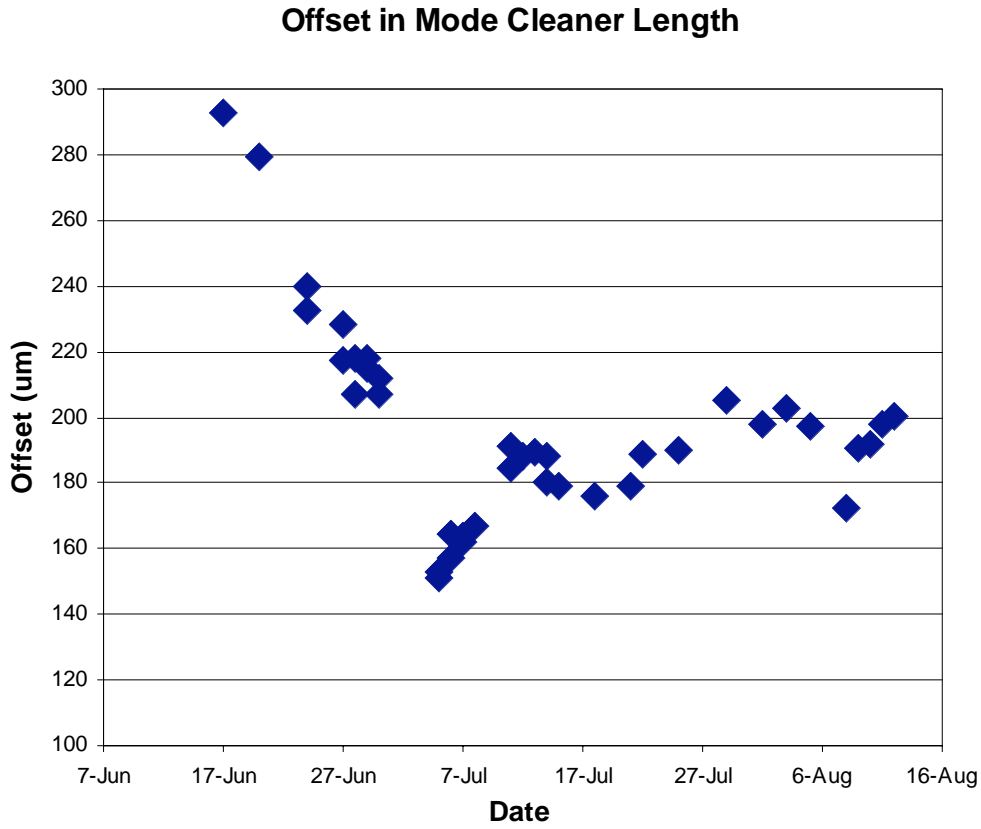


**Fig. 1 – Plot of Daily Measurements of the Mode Cleaner Length. Over the course of the 10-week study, the MC length has drifted by approximately 100 $\mu\text{m}$ . The drift has brought the RF sidebands closer to resonance.**

Thermal expansion of the concrete floor from the unintentional rise in temperature is suggested as a cause of the original 300  $\mu\text{m}$  offset in the length. After the temperature reduction, the MC steadily shortened until leveling off in early July. Figure 2 shows the temperature in the LVEA during this period.

In addition, the ITMX and ITMY optical lever pier temperatures were taken with each daily measurement. The channels LVE-EX:ETMX\_OP\_LEV\_TEMP and LVE-EY:ETMY\_OP\_LEV\_TEMP were used for the readouts. Since the new temperature sensors were installed on June 27<sup>th</sup>, the temperature readouts have remained within  $\pm 0.5^\circ\text{C}$ . During this same time period, the mode cleaner length varied by almost 100  $\mu\text{m}$ , and we observed no correlation between the optical lever temperature and MC length. Figure 3 shows a graph of the ITMX optical level temperature readout and the drift in the mode cleaner length from June 27<sup>th</sup> to August 7<sup>th</sup>.

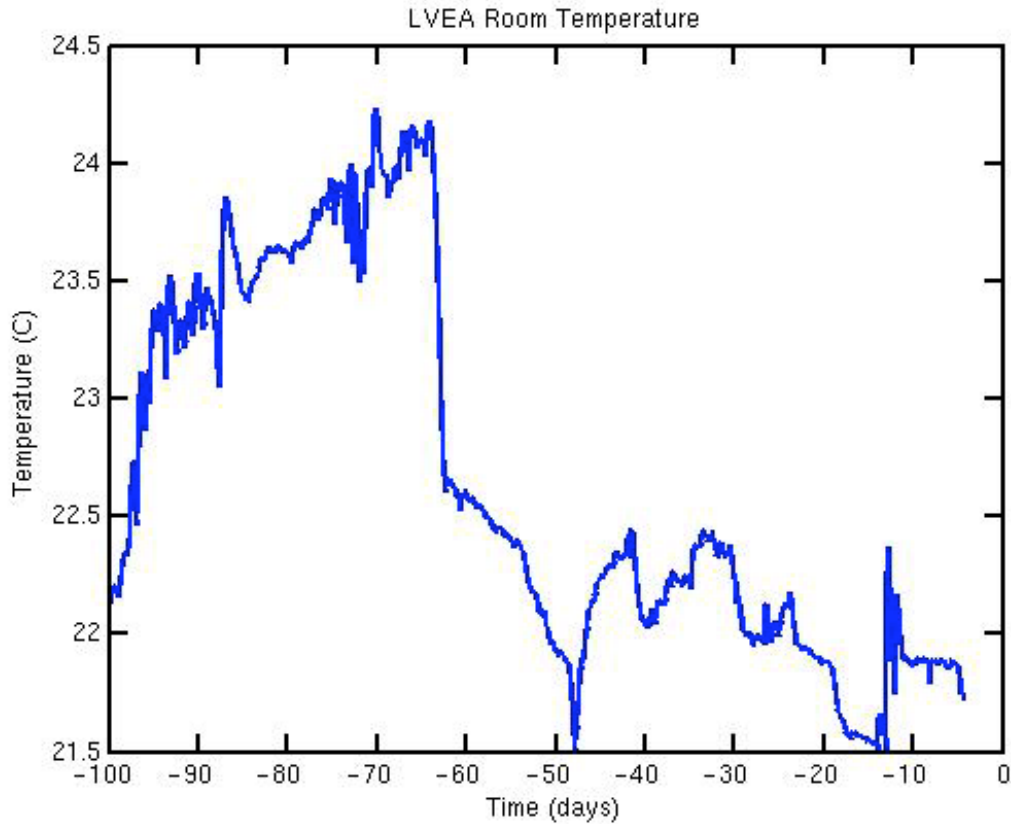


**Fig. 2 – Plot of LVEA Temperature over 100 days prior to 8/16/05. Data taken from the L1:PSL-FSS\_RMTEMP channel. The temperature sensors were recalibrated on June 16th causing a drop of about 3°C in the LVEA. This may explain the 100-150 $\mu$ m drift in the MC length over the next 3 weeks.**

We also examined the role of motion of the mode cleaner optics relative to the frame. Data was taken from the L1:SUS-MC\_URPDMon channels and calibrated to give relative tilt in millimeters. Aside from spikes during times when HEPI was down, the long-term relative motion was within  $\sim 10 \mu\text{m}$  for all three mirrors. Figure 4 shows the motion of MC1 from July 5<sup>th</sup> through July 23<sup>rd</sup>, which displayed the most long-term movement among the MC optics. The data was plotted by hour average.

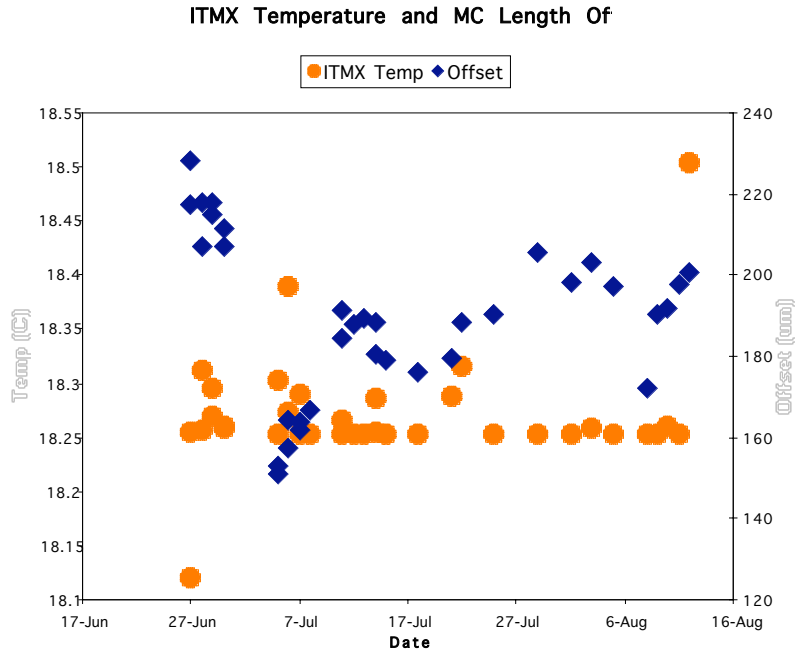


**Fig. 3 – Plot of ITMX Optical Lever Temperature and MC Length. Over the 7-week period shown above, the temperature readout remained within 0.5C while the mode cleaner length drifted by nearly 100um.**

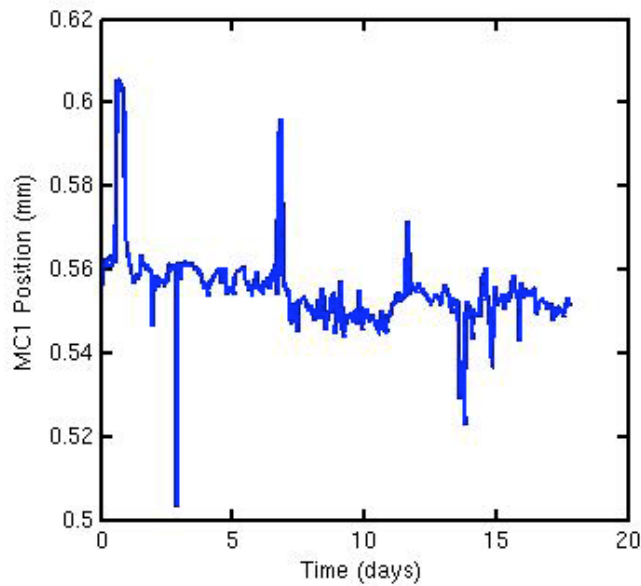


**Fig. 4 –Motion of MC1 Relative to Frame. Plot displays data from the L1:SUS-MC1\_URPDMon channel from July 5th through 23rd. This channel monitors the tilt of the MC1 mirror relative to the frame. Relative motion accounts ~10μm over the course of many days.**

## **IMPACT ON NOISE**

In the same way the measured beat signal is transmitted through the cavity, oscillator phase noise can appear as amplitude modulation of the RF sidebands in the light coming out of the mode cleaner [2].

We examined the effect of offset in the mode clear length on RF AM noise by measuring the power spectrum of the light on the LSC\_REFL photo detector in the kHz range. At a measured offset of 192  $\mu\text{m}$ , we varied the PD DC voltage and looked for any noticeable appearance of noise above the shot noise that dominates in that band. We found no excess above the shot noise, and conclude that the RFAM RIN is dominated by the shot noise from the 20 mA photocurrent.

Additionally, when the first measurements revealed a change in length of  $\sim 300 \mu\text{m}$  from RF sideband resonance, HEPI was shifted by 300  $\mu\text{m}$  to compensate [3]. However, there was no noticeable change in the IFO performance, so HEPI was returned to zero offset.

## **CONCLUSIONS**

The length of the mode cleaner can drift on the order of 100  $\mu\text{m}$  over the course of several weeks. The most likely explanation for long-term drift of this magnitude is temperature change in the LVEA, causing thermal expansion of the concrete floor and lengthening the mode cleaner cavity. While a number of other factors have been suggested as causes of drift mode cleaner length, such as temperature changes in other locations or motion of the optics relative to the frame, no clear correlations were found.

At present, the  $\sim 200 \mu\text{m}$  offset from RF sideband resonance does not have a noticeable impact on the performance of the interferometer. The RF amplitude modulation in the mode cleaner transmitted beam caused by offset from sideband resonance is dominated by the shot noise of current across the photo detectors. However, though length change of this magnitude does not produce a marked effect on noise in the IFO dark port signal, it may become more important in the future as noise levels are further reduced or preparations are made for Advanced LIGO.

## REFERENCES

1. Weiss, Rai. "Change in LVEA Temp," LIGO Livingston Detector Group E-log. [http://ilog.ligo-la.caltech.edu/ilog/pub/ilog.cgi?group=detector&date\\_to\\_view=06/16/2005&anchor\\_to\\_scroll\\_to=2005:06:16:17:14:09-RaiW](http://ilog.ligo-la.caltech.edu/ilog/pub/ilog.cgi?group=detector&date_to_view=06/16/2005&anchor_to_scroll_to=2005:06:16:17:14:09-RaiW)
2. Adhikari, Rana. "Sensitivity and Noise Analysis of 4 km Laser Interferometric Gravitational Wave Antennae." Ph.D. Thesis, Massachusetts Institute of Technology, July 2004.
3. Frolov, Valera. "IFO Locking," LIGO Livingston Detector Group E-log. [http://ilog.ligo-la.caltech.edu/ilog/pub/ilog.cgi?group=detector&date\\_to\\_view=06/16/2005&anchor\\_to\\_scroll\\_to=2005:06:16:03:43:00-valera](http://ilog.ligo-la.caltech.edu/ilog/pub/ilog.cgi?group=detector&date_to_view=06/16/2005&anchor_to_scroll_to=2005:06:16:03:43:00-valera)
4. J. B. Camp, H. Yamamoto, S. E. Whitcomb. "Analysis of Light Noise Sources in a Recycled Michelson Interferometer with Fabry-Perot Arms," J. Opt. Soc. Am. Vol. 17, No. 1 January 2000.



## APPENDIX – Derivation of the Measured Beat Signal

The carrier field, oscillating at frequency  $\omega_c$ , is phase modulated at the RF frequency  $\Omega \cong 25$  MHz. We impose an additional frequency modulation at  $\omega_m \cong 633$  Hz. The light entering the mode cleaner is described by

$$E_{IN} = E_0 e^{i(\omega_c(1+\alpha \cos(\omega_m t))t + \beta \cos(\Omega t))} \cong E_0 e^{i\omega_c t} [1 + i\alpha\omega_c \cos(\omega_m t)][1 + i\beta \cos(\Omega t)]$$

where  $\alpha$  and  $\beta$  are the modulation depths of the audio and RF sidebands, respectively. This results in additional audio sidebands around both the carrier and the RF sidebands, for a total of 9 fields:

$$\cong E_0 e^{i\omega_c t} \left[ \begin{aligned} &1 + \frac{i\alpha\omega_c}{2} e^{i\omega_m t} + \frac{i\alpha\omega_c}{2} e^{-i\omega_m t} + \frac{i\beta}{2} e^{i\Omega t} + \frac{i\beta}{2} e^{-i\Omega t} \\ &- \left( \frac{\alpha\beta\omega_c}{4} \right) e^{i(\omega_m + \Omega)t} - \left( \frac{\alpha\beta\omega_c}{4} \right) e^{i(\omega_m - \Omega)t} - \left( \frac{\alpha\beta\omega_c}{4} \right) e^{i(-\omega_m + \Omega)t} - \left( \frac{\alpha\beta\omega_c}{4} \right) e^{i(-\omega_m - \Omega)t} \end{aligned} \right]$$

The light passes through the mode cleaner and each of the fields picks up a factor of the MC transfer function [4],

$$T(\Delta\omega) = \frac{E_{IN}}{E_{OUT}} = \frac{it^2 e^{-i\Delta\omega L/c}}{1 - r^2 e^{-i2\Delta\omega L/c}},$$

where  $\Delta\omega$  is the distance (in frequency) from the carrier and  $L$  is the round-trip length of the mode cleaner cavity. After multiplying each term by the mode cleaner transfer function evaluated at that frequency, the current through the MC Trans photodiode is proportional to the magnitude-squared of the total field. The signal in the REFL-Q channel is demodulated using the RF oscillator signal and the result is proportional to

$$I_{DEMOD} \propto i\alpha\beta\omega_c \left[ \left( \frac{t^4 e^{-i(\omega_m - \Omega)L/c}}{(1 - r^2 e^{-i2\omega_m L/c})(1 - r^2 e^{i2\Omega L/c})} - \frac{t^4 e^{-i(\omega_m + \Omega)L/c}}{(1 - r^2 e^{-i2\omega_m L/c})(1 - r^2 e^{-i2\Omega L/c})} \right) - C.C. \right]$$

The important result is that the signal is linear with length changes on the order of hundreds of micrometers and vanishes when the RF sidebands are on resonance. We verified this by plotting the above expression in Mathematica using the nominal values of each parameter [4].

## APPENDIX – Plots of Derived Signal

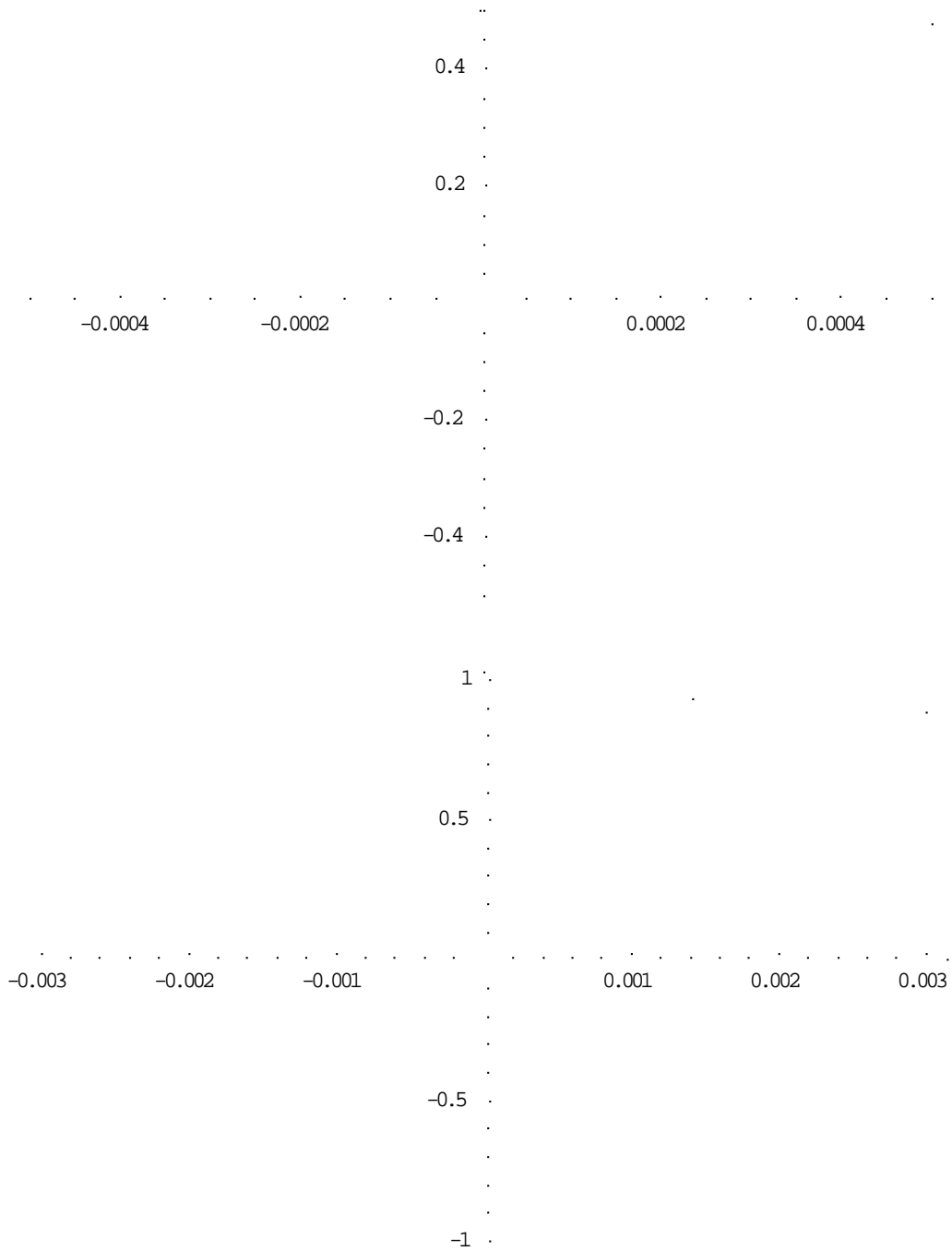


**Figure 5 – Plots of the Analytic Expression for the Measured Beat Signal. Horizontal axis shows offset in the MC length (in meters). Vertical axis shows magnitude of the transfer function to within a constant of proportionality.**

## APPENDIX –Table of Measured Data

Date	Time	Magnitude Q	Phase Q	Coherence Q	DC Mon	DC/Gain Adjusted Magnitude	Offset (um)
17-Jun	13:21	0.539357	-117.87	0.999402	1.65572	0.567990755	292.4398919
20-Jun	16:20	0.479094	-117.896	0.998973	1.53853	0.542958461	279.5458123
24-Jun	10:20	0.465528	-118.794	0.999254	1.74362	0.465528	239.6615524
24-Jun	16:00	0.474933	-118.025	0.999197	1.83151	0.452142045	232.7664766
27-Jun	10:40	0.460643	-117.116	0.99906	1.81198	0.443264466	228.1936552
27-Jun	16:20	0.434981	-117.342	0.999135	1.79733	0.421982369	217.2312937
28-Jun	10:40	0.456109	-118.68	0.999229	1.88034	0.422945199	217.7272451
28-Jun	16:40	0.428306	-118.422	0.998809	1.85592	0.402389601	207.1391018
29-Jun	10:00	0.41712	-119.184	0.999176	1.7192	0.42304489	217.7785958
29-Jun	13:30	0.417935	-118.236	0.999398	1.74362	0.417935	215.1465028
30-Jun	11:20	0.429508	-118.251	0.999324	1.82174	0.411089804	211.6205573
30-Jun	16:30	0.417541	-118.379	0.99913	1.81198	0.401788562	206.8295081
5-Jul	10:15	0.421363	-118.238	0.998683	1.98777	0.40773891	152.855672
5-Jul	16:45	0.473088	-118.643	0.999242	2.01218	0.40305749	151.0993612
6-Jul	10:00	0.471062	-118.055	0.998406	1.84128	0.438581317	164.4267026
6-Jul	13:30	0.458657	-117.652	0.998906	1.87546	0.419249074	157.1738972
7-Jul	9:45	0.488421	-118.826	0.999428	1.93894	0.431838989	161.8972084
7-Jul	15:25	0.450408	-117.976	0.998873	1.76803	0.436725306	163.7303898
8-Jul	16:15	0.464098	-118.07	0.999473	1.78756	0.445082953	166.8658969
11-Jul	11:00	0.510361	-118.247	0.999373	1.71432	0.510361	191.3560177
11-Jul	16:00	0.505016	-118.026	0.999513	1.75826	0.492395339	184.6159079
12-Jul	13:40	0.490228	-118.329	0.999406	1.67525	0.501661045	188.092088
13-Jul	10:15	0.49971	-118.772	0.999396	1.69479	0.505468434	189.520492
14-Jul	10:15	0.510553	-117.907	0.999358	1.74362	0.501973606	188.2093505
14-Jul	15:15	0.516384	-118.261	0.999419	1.84128	0.480778273	180.2575767
15-Jul	16:15	0.495806	-118.065	0.999528	1.7778	0.478102229	179.2536151
18-Jul	16:15	0.48498	-118.255	0.999085	1.77291	0.46895269	175.8210169
21-Jul	14:30	0.505525	-118.279	0.986025	1.81198	0.478278799	179.3198583
22-Jul	10:40	0.494117	-119.014	0.999105	1.68502	0.502708962	188.4852313
25-Jul	14:15	0.507311	-118.492	0.999114	1.71432	0.507311	190.2117606
29-Jul	15:00	0.555446	-118.304	0.999353	1.73873	0.547648103	205.3448808
1-Aug	13:00	0.526906	-118.495	0.998948	1.70943	0.528413269	198.1286198
3-Aug	16:20	0.533723	-118.857	0.995831	1.6899	0.541435596	203.0141576
5-Aug	10:15	0.527186	-118.32	0.999247	1.7192	0.525689567	197.1067788
8-Aug	16:00	0.490283	-119.017	0.999411	1.83151	0.458912019	172.0540961
9-Aug	13:20	0.513917	-118.687	0.999577	1.73385	0.508128265	190.5183707
10-Aug	14:45	0.512075	-118.349	0.999486	1.71432	0.512075	191.9990527
11-Aug	10:00	0.541043	-118.068	0.999341	1.75826	0.527522002	197.7942467
12-Aug	10:45	0.537646	-118.429	0.999364	1.7235	0.534782298	200.5180647

**Table 2 – Selected Measured Data from Daily Measurements. Other recorded data included the REFL-I transfer function, ITMX and ITMY optical level pier temperatures, and relevant gain readouts.**